Heterogeneous Catalysis

DOI: 10.1002/ange.201408896

Chiral Metal–Organic Frameworks Bearing Free Carboxylic Acids for Organocatalyst Encapsulation**

Yan Liu, Xiaobing Xi, Chengcheng Ye, Tengfei Gong, Zhiwei Yang, and Yong Cui**

Abstract: *Two chiral carboxylic acid functionalized micro- and mesoporous metal–organic frameworks (MOFs) are constructed by the stepwise assembly of triple-stranded heptametallic helicates with six carboxylic acid groups. The mesoporous MOF with permanent porosity functions as a host for encapsulation of an enantiopure organic amine catalyst by combining carboxylic acids and chiral amines in situ through acid–base interactions. The organocatalyst-loaded framework is shown to be an efficient and recyclable heterogeneous catalyst for the asymmetric direct aldol reactions with significantly enhanced stereoselectivity in relative to the homogeneous organocatalyst.*

Metal–organic frameworks (MOFs) provide a unique opportunity to design and synthesize functional crystalline porous materials for diverse applications from organic struts and metal ions.[1,2] Owing to their hybrid composition, modularity, high surface areas and tunable porosity, MOFs have been targeted as particularly attractive supports for molecular catalysts,[3] and especially for asymmetric reactions that cannot be realized with traditional porous inorganic and organic materials.[4–6] Chiral MOF catalysts are typically made from metal ions and functionalized privileged chiral ligands such as BINOL and salen,[7,8] but it is challenging for this direct approach to build MOFs from organic catalysts because they are often the ligating functionality of choice for framework construction.[6,9] Alternatively, the introduction of chiral auxiliaries with reactive binding sites inside MOFs may be achieved by post-synthetic modification.[10] In this approach, the synthesis of MOFs with desired functionalities, stability, and pore sizes seems to be within reach. Nonetheless, there are only several reports of MOFs that displayed enantiopure organocatalysis.[6]

Asymmetric organocatalysis has emerged as a powerful synthetic method that is complementary to metal- and enzyme-catalyzed transformations.[11] In particular, acid–base assembly of chiral amines is one of the most efficient bifunctional enamine catalysts.[12] The acids utilized in these cases were essential units that dramatically impacted the catalytic activity and stereoselectivity.[13] Based on the acid–base principle, it should be effective for supporting chiral amine in MOFs with channels decorated with free carboxylic acids, which may play a dual role as catalyst anchors and modulators for activity and stereoselectivity. However, MOFs with struts containing free carboxylic acids remain rare.[14] We have recently described the assembly of a pyridyl-functionalized cluster helicate into MOFs, but which lack binding functional groups.[15] Herein we report the synthesis of a carboxylic acid functionalized triple-stranded helicate to build micro- and mesoporous MOFs having free carboxylic groups. Encapsulation of a chiral amine in the mesoporous MOF led to a recyclable heterogeneous catalyst for the asymmetric direct aldol reactions with significantly enhanced stereoselectivity.

The ligand H_4**L**-(2MOM) (MOM = methoxymethyl) was synthesized in 80% yield by the Schiff-base condensation of 5-*tert*-butyl-3-(4-carboxylic acid)salicylaldehyde and enantiopure 3,3′-diamino-5,5′,6,6′-tetramethyl-2,2′-methoxymethyl-1,1′-biphenyl. Treatment of H_4**L**-(2MOM) and $Zn(ClO_4)_2\cdot 6H_2O$ in a 1:3 molar ratio in DMF and MeOH at 80 °C afforded $[Zn_7(H_2\mathbf{L})_3(OMe)_2]\cdot H_2O$ (**1**) in 75% yield (Scheme 1). Heating **1** and $Cd(NO_3)_2\cdot 4H_2O$ and $Zn(NO_3)_2\cdot 6H_2O$ (1:2 molar ratio) in DMF and pyridine at 100 °C afforded $[Cd_2\{Zn_7\mathbf{L}(H\mathbf{L})_2(OH)_2\}(Py)_2(H_2O)]\cdot$DMF (**2**) and $[Zn_4O]_{2/3}[Zn_7\mathbf{L}_2(H_2\mathbf{L})(OH)_2]\cdot 3H_2O$ (**3**), respectively (see the Supporting Information). Compounds **2** and **3** are stable in air and insoluble in water and common organic solvents. The formulations were supported by elemental analysis and single-crystal X-ray diffraction (XRD) analysis. The phase purity of the bulk samples was confirmed by their powder XRD patterns.

Compound **1** crystallizes in the chiral trigonal space group *R*3 and adopts a heptanuclear helical structure.[16] The MOM groups were removed from the ligands upon complexation with Zn ions, and each **L** binds to two Zn ions through two tridentate N + 2O donors and to another two Zn through two biphenolate oxygen atoms. Seven Zn ions thus formed two Zn_4O_4 distorted cubanes by sharing one Zn ion. Each of the six outer Zn ions is square-pyramidally coordinated by three O and one N atoms from two **L** ligands and one OMe anion, while the central Zn ion is octahedrally coordinated to three O and three N atoms from three **L** ligands. The cluster can be viewed as an *M*-configured triple-stranded helicate that has perfect D_3 point-group symmetry, with one crystallographic C_3 axis running through two μ_3-$^-$OMe units and three

[*] Prof. Y. Liu, Dr. X. Xi, C. Ye, T. Gong, Z. Yang, Prof. Y. Cui
School of Chemistry and Chemical Engineering and
State Key Laboratory of Metal Matrix Composites
Shanghai Jiao Tong University, Shanghai 200240 (China)
E-mail: liuy@sjtu.edu.cn
yongcui@sjtu.edu.cn
Prof. Y. Cui
Collaborative Innovation Center of Chemical Science and Engineering
Tianjin 300072 (China)

[**] This work was supported by the NSFC (21025103, 21371119, 21431004, and 21401128), "973" Program (2014CB932102 and 2012CB8217), and SSTC-12XD1406300 and 14YF1401300.

Supporting information for this article is available on the WWW under http://dx.doi.org/10.1002/anie.201408896.

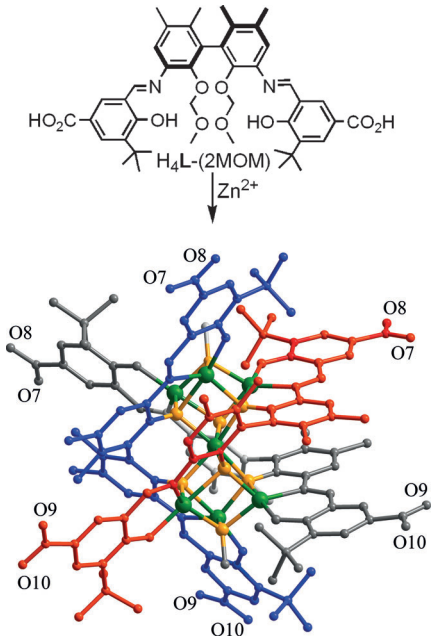

Scheme 1. Synthesis of helicate **1**. MOM = methoxymethyl.

crystallographic C_2 axes bisecting three opposite **L** edges. Complex C–H···O interactions and hydrophobic interactions direct packing of helicates along the *ab* plane forming a 2D framework. Such 2D grids stack on top of each other along the *c*-axis to form a 3D supramolecular structure with an opening size of about 1.7 nm × 1.6 nm along the [211] direction.

Compound **2** crystallizes in the chiral orthorhombic space group $I2_12_12_1$. The Zn_7 cluster adopts almost the same helicate structure as in **1**, but with the μ_3-$^-$OMe bridges replaced by μ_3-OH^- anions. The helicate acts as a tetradentate ligand, binding to four Cd ions using four of its six carboxylate groups in a chelating fashion (Figure 1). Of the two independent Cd ions, the Cd1 is octahedrally coordinated by two pyridine molecules and two bidentate carboxylate groups from two different Zn_7 helicates, and the Cd2 is heptahedrally coordinated by one water, two pyridine, and two bidentate carboxylate groups from two Zn_7 helicates. Along the *a*-axis, adjacent helicates are linked by the Cd1 ions to form a left-handed 2_1 helix with a pitch of 1.75150(19) nm, a pair of which associate in parallel forming a tube with an opening of about 0.24 × 0.34 nm. Four such tubes are linked by the Cd2 to give a 1D channel of about 0.20 × 0.54 nm with the CO_2H groups pointing to Cd centers. The helicates are thus linked by two kinds of Cd ions to form a chiral 3D network functionalized with carboxylic groups.

Compound **3** crystallizes in the chiral hexagonal space group $P6_322$. Again, the Zn_7 helicate acts as a tetradentate ligand and binds to four newly generated well-known [$Zn_4(\mu_4$-O)] clusters using four of its six carboxylate groups in a bidentate fashion. In the Zn_4O core, the Zn ions are each tetrahedrally coordinated to one μ_4-O anion and three carboxylate oxygen atoms from three Zn_7 helicates. As a result, each Zn_7 helicate binds to four Zn_4O via four bidentate carboxylate groups, whereas each Zn_4O connects six Zn_7 helicates to form a (4,6)-connected 3D framework with 1D chiral hexagonal channels along the *a*-axis, which are periodically decorated with pairs of six uncoordinated CO_2H groups that are related by the crystallographic six-fold axis (Figure 2). The 1D channel can also be viewed as being composed of a number of cylindrical cages with D_6 symmetry, each of which is enclosed by twelve Zn_7 helicates and six Zn_4O clusters. The cage has a height of about 1.4 nm and a maximum inner width of about 2.36 nm (considering van der Waals radii). The hexagonal apertures that surround by six free carboxylic groups on the top and bottom faces have a diagonal distance of about 1.6 nm × 1.4 nm.

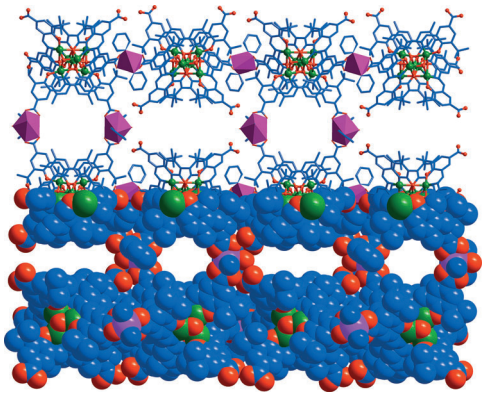

Figure 1. Space-filling and stick model of **2** viewed along the *c*-axis, with different channel sizes owing to different distributions of the ligands.

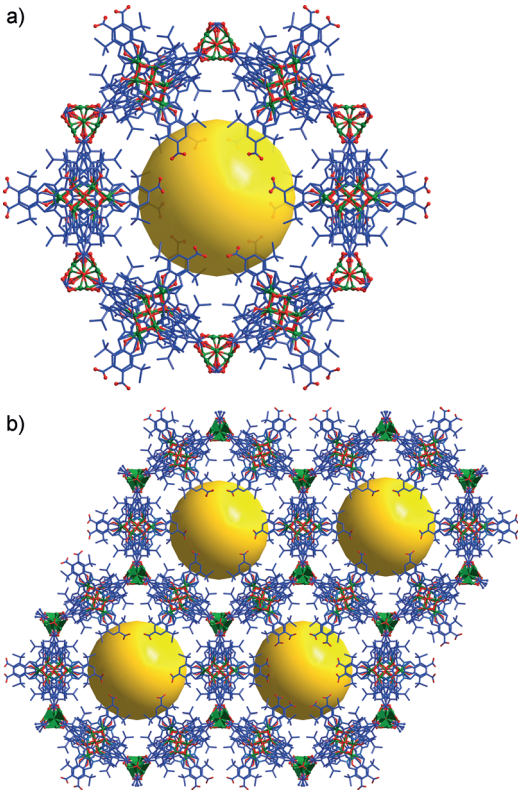

Figure 2. a) The mesoporous cage and b) the 3D porous network in **3** viewed along the *c*-axis.

ESI-MS showed that helicate **1** was stable in DMF, as evidenced by a prominent signal at $m/z = 2549.5$ that is due to $[Zn_7(OH)_2\mathbf{L}_3{+}H]^+$ (Supporting Information, Figure S17). Both UV/Vis and CD spectra of **1** are almost the same at room temperature and 80 °C in DMF, indicating the good stability of the helical structure and its optical activity during MOF crystallization. The key factor for the formation of the CO_2H-functionalized MOFs may be due to steric crowding around the CO_2H positions in the Zn_7 helicate, which prevented some of the carboxylic acid groups from participating in the metal coordination.[14e] Solid-state CD spectra of **1**–**3** made from *R* and *S* enantiomers of H_2**L**-(2MOM) are mirror images of each other, indicative of their enantiomeric nature. TGA revealed that the solvent molecules could be removed from **1**–**3** in the 80–150 °C range. PXRD showed that they retain their structural integrity and crystallinity upon guest removal (Supporting Information, Figures S4–S6).

Calculations using PLATON indicate that **1**–**3** have 49.3, 50.2, and 68.5 % of total volume occupied by solvent molecules, respectively.[17] The N_2 sorption measurements at 77 K showed that the apohost **3** exhibit a pseudo-type-II sorption behavior with a BET surface area of 1015.5 $m^2 g^{-1}$. The pore size distribution calculated using nonlocal density functional theory is centered at about 2.3 nm, consistent with the result of single-crystal X-ray diffraction (Supporting Information, Figure S11). In contrast, **1** and **2** only exhibit surface sorption. Interestingly, **3** could readily adsorb 3.2 Rhodamin 6G molecules (ca. 1.4 nm × 1.6 nm in size) and 1.1 Brilliant Blue R-250 molecules (1.8 nm × 2.2 nm in size) per formula unit in MeOH. The inclusion solids exhibited similar PXRD patterns to the pristine sample, but a structural distortion occurred (Supporting Information, Figure S7), suggesting that the structural integrity and open mesochannels of **3** are maintained in solution. To our knowledge, **2** and **3** are the first two examples of chiral MOFs containing free CO_2H groups that are beneficial for enantioselective recognition.[14]

Pyrrolidine derivatives are widely used as organocatalysts for a variety of organic transformations, such as the aldol reaction.[18] The presence of free CO_2H groups in **2** and **3** has prompted the inclusion of a pyrrolidine catalyst for catalysis. After many attempts, it was found that (*S*)-2-(dimethylaminomethyl) pyrrolidine, (*S*)-Ap, could be entrapped by **3** by solution adsorption (Scheme 2). The adduct Ap@**3** was achieved by soaking the evacuated MOF in a dilute anhydrous THF solution of Ap for two days at 0 °C. After this treatment, the crystals remained transparent but with apparent fracturing. The formation of a 1:1 host–guest complex was suggested by GC, TGA, and elemental analysis. The PXRD pattern was nearly identical to that of the parent MOF, indicating that the adsorption

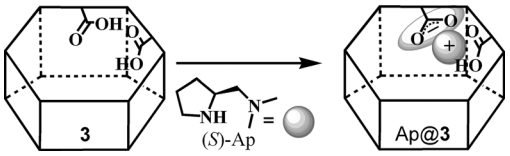

Scheme 2. Synthesis of Ap@**3** by post-modification. The hexagonal cage in **3** is shown as a hexagonal prism.

was not detrimental to the crystal structure. Ap@**3** gave a decreased BET surface area (354.6 $m^2 g^{-1}$) compared with **3**. However, the addition of **2** into a solution of Ap led to the framework decomposition.

After optimization of reaction conditions, Ap@**3** was found to be an active catalyst for the direct aldol reaction of both acetone and cyclohexanone with nitro-substituted aromatic aldehydes in a ketone/water (1:0.05 molar ratio) mixture. Especially, 10 mol % loading of (*S*/*S*)-Ap@**3** catalyzes the reaction of acetone with 4-nitrobenzaldehyde and 3-nitrobenzaldehyde to afford the products in 80 and 74 % *ee* and 77 and 73 % yield of isolated product, respectively, at room temperature after 48 h. The catalytic reaction also worked well with cyclohexanone, affording the products in 74 and 66 % *ee*, 72 and 68 % yield, and 3.3:1.0 and 2.0:1.0 *anti*/*syn* ratio, respectively. A control experiment with MOF **3** afforded about 10 % conversion of 4-nitrobenzaldehyde but with less than 5 % *ee* after 48 h, presumably catalyzed by the free carboxylic acids. The reaction between 4-nitrobenzaldehyde and acetone catalyzed by either (*S*/*R*)-Ap@**3** or a mixture of (*S*/*S*)-Ap@**3** and (*S*/*R*)-Ap@**3** (a 1:1 molar ratio) gave the *R* over the *S* enantiomer (ca. 80 % *ee*) as well, suggesting that the solid catalyst relies on the intrinsic chiral nature of the organocatalyst Ap to exert stereocontrol.

To study the confinement effect of a MOF on the organic catalyst, the activity of Ap was assessed. At 10 mol % catalyst loadings, Ap afforded the desired aldol products in 48–64 % *ee* and 71–79 % yield of isolated product (Table 1, entries 2, 4, 6, and 8) in the presence of benzoic acid.[18] The catalysis by Ap was significantly accelerated by benzoic acid, as it may

Table 1: Direct aldol reactions catalyzed by Ap@**3** and Ap.[a]

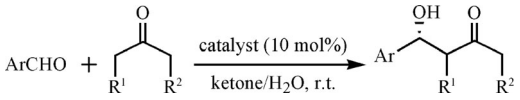

Entry	Catalyst[b]	Ar	R^1/R^2	Yield [%][c]	*anti*/*syn*[d]	*ee* [%][e,f]
1	Ap@**3**	4-NO_2Ph	H/H	77(76)[g]	–	80 (80)[g]
2	Ap[h]	4-NO_2Ph	H/H	79	–	64
3	Ap@**3**	3-NO_2Ph	H/H	73	–	74
4	Ap[h]	3-NO_2Ph	H/H	76	–	56
5	Ap@**3**	4-NO_2Ph	$-(CH_2)_3-$	72	3.3/1.0	74[i]
6	Ap[h]	4-NO_2Ph	$-(CH_2)_3-$	75	2.9/1.0	48[i]
7	Ap@**3**	3-NO_2Ph	$-(CH_2)_3-$	68	2.0/1.0	66[i]
8	Ap[h]	3-NO_2Ph	$-(CH_2)_3-$	71	1.9/1.0	50[i]

[a] For reaction details see the Experimental Section in the Supporting Information. [b] (*S*/*S*)-Ap@**3** or (*S*)-Ap was used as the catalyst unless otherwise noted. [c] The yield of the isolated product based on aldehyde. [d] Determined by ^{1}H NMR spectroscopy from the crude reaction mixture. [e] Determined by HPLC. [f] The absolute configuration (*R*) was assigned by comparing the retention time with that of the standard sample. [g] (*S*/*R*)-Ap@**3** was used as the catalyst. [h] One equivalent of benzoic acid was used. [i] Value represents the major isomer.

provide a proton to accelerate the formation of enamine. Therefore, the *ee* values observed for Ap@**3** are significantly higher than those for the Ap homogeneous control, whereas the yields and the diastereoselectivity are comparable to those for the homogeneous control, although the heterogeneous reactions required longer time because of their slow mass diffusion. A variety of solid-supported chiral amine catalysts have been developed for the aldol reactions, but they are typically less effective than their homogeneous analogues.[19] MOF-catalyzed aldol reactions, including several asymmetric reactions with moderate to good enantioselectivity (up to 80% *ee*), have also been documented.[5a,6a–c,20] The present improved enantioselection may arise from the restricted movement of the substrates in the porous structure in combination with multiple chiral inductions.

To study whether the catalysis by Ap@**3** occurred predominantly within the pores or just on the surface, a sterically more demanding substrate 5-formyl-1,3-phenylenebis(3,5-di-*tert*-butylbenzoate) was subjected to the aldol reaction. Less than 10% conversion was obtained after 48 h, which is much lower than the more than 53% conversion obtained by using Ap. This result suggested that this bulky substrate cannot access the catalytic sites. It is thus likely that the catalytic reactions occur within the MOF.

The supernatant from the reaction of 3-nitrobenzaldehyde and acetone after filtration through a regular filter did not afford any obvious product, suggesting the heterogeneous nature of the reaction. Upon completion of the reaction, Ap@**3** could be readily recovered by centrifugation and reused for the next cycle without significant loss of activity and enantioselectvity. The yield/*ee* values for the three consecutive runs are 73/74%, 72/73% and 70/73%, respectively. PXRD showed that the recycled sample retained high crystallinity after three runs, although the structure became slightly distorted (Supporting Information, Figure S8). GC and ICP-OES analyses indicated no leaching of Ap and zinc ions ($\approx$0.005%), respectively, from the framework per cycle.

In conclusion, we have described the synthesis of two chiral porous MOFs functionalized with carboxylic acid groups. After encapsulating an organic amine, the mesoporous framework was shown to be an efficient and recyclable heterogeneous catalyst for the asymmetric direct aldol reactions that exhibited markedly improved catalytic performance relative to its homogeneous counterpart. The acid–base procedure for guest inclusion enables the use of the native catalysts without modification of the ancillary ligands and/or MOF linkers, and, taking advantage of this strategy, more MOF-based catalysts can be expected to be discovered.

Received: September 8, 2014
Published online: November 7, 2014

Keywords: aldol reactions · heterogeneous catalysis · metal–organic frameworks · organocatalysis · porous materials

[1] a) L. E. Kreno, K. Leong, O. K. Farha, M. Allendorf, R. P. V. Duyne, J. T. Hupp, *Chem. Rev.* **2012**, *112*, 1105–1125; b) Y. Inokuma, M. Kawano, M. Fujita, *Nat. Chem.* **2011**, *3*, 349–358; c) H. Furukawa, K. E. Cordova, M. O'Keeffe, O. M. Yaghi, *Science* **2013**, *341*, 1230444.

[2] a) D. Bradshaw, J. B. Claridge, E. J. Cussen, T. J. Prior, M. J. Rosseinsky, *Acc. Chem. Res.* **2005**, *38*, 273–282; b) N. Stock, S. Biswas, *Chem. Rev.* **2012**, *112*, 933–969; c) T. R. Cook, Y.-R. Zheng, P. J. Stang, *Chem. Rev.* **2013**, *113*, 734–777.

[3] a) D. Farrusseng, S. Aguado, C. Pinel, *Angew. Chem. Int. Ed.* **2009**, *48*, 7502–7513; *Angew. Chem.* **2009**, *121*, 7638–7649; b) A. Corma, H. Garcia, F. X. L. I. Xamena, *Chem. Rev.* **2010**, *110*, 4606–4655.

[4] a) J. Lee, O. K. Farha, J. Roberts, K. A. Scheidt, S. T. Nguyen, J. T. Hupp, *Chem. Soc. Rev.* **2009**, *38*, 1450–1459; b) L. Ma, C. Abney, W. Lin, *Chem. Soc. Rev.* **2009**, *38*, 1248–1256; c) Y. Liu, W. Xuan, Y. Cui, *Adv. Mater.* **2010**, *22*, 4112–4135; d) M. Yoon, R. Srirambalaji, K. Kim, *Chem. Rev.* **2012**, *112*, 1196–1231.

[5] a) K. Gedrich, M. Heitbaum, A. Notzon, I. Senkovska, R. Fröhlich, J. Getzschmann, U. Mueller, F. Glorius, S. Kaskel, *Chem. Eur. J.* **2011**, *17*, 2099–2106; b) M. J. Ingleson, J. P. Barrio, J. Bacsa, C. Dickinson, H. Park, M. J. Rosseinsky, *Chem. Commun.* **2008**, 1287; c) K. S. Jeong, Y. B. Go, S. M. Shin, S. J. Lee, J. Kim, O. M. Yaghi, N. Jeong, *Chem. Sci.* **2011**, *2*, 877–882.

[6] a) D. J. Lun, G. I. N. Waterhouse, S. G. Telfer, *J. Am. Chem. Soc.* **2011**, *133*, 5806–5809; b) M. Banerjee, S. Das, M. Yoon, H. J. Chois, M. H. Hyun, S. M. Park, G. Seo, K. Kim, *J. Am. Chem. Soc.* **2009**, *131*, 7524–7525; c) D. Dang, P. Wu, C. He, Z. Xie, C. Duan, *J. Am. Chem. Soc.* **2010**, *132*, 14321–14323; d) P. Wu, C. He, J. Wang, X. Peng, X. Li, Y. An, C. Duan, *J. Am. Chem. Soc.* **2012**, *134*, 14991–14999; e) M. Zheng, Y. Liu, C. Wang, W. Lin, *Chem. Sci.* **2012**, *3*, 2623; f) Z. Zhang, Y. R. Ji, L. Wojtas, W. Gao, S. Ma, M. J. Zaworotko, J. C. Antilla, *Chem. Commun.* **2013**, *49*, 7693–7695.

[7] a) S. H. Cho, B. Q. Ma, S. T. Nguyen, J. T. Hupp, T. E. Albrecht-Schmitt, *Chem. Commun.* **2006**, 2563–2565; b) F. Song, C. Wang, J. M. Falkowski, L. Ma, W. Lin, *J. Am. Chem. Soc.* **2010**, *132*, 15390–15398; c) J. M. Falkowski, C. Wang, S. Liu, W. Lin, *Angew. Chem. Int. Ed.* **2011**, *50*, 8674–8678; *Angew. Chem.* **2011**, *123*, 8833–8837; e) C. Zhu, G. Yuan, X. Chen, Z. Yang, Y. Cui, *J. Am. Chem. Soc.* **2012**, *134*, 8058–8061; d) M. C. Das, Q. Guo, Y. He, J. Kim, C. Zhao, K. Hong, S. Xiang, Z. Zhang, K. M. Thomas, R. Krishna, B. Chen, *J. Am. Chem. Soc.* **2012**, *134*, 8703–8710.

[8] a) K. Tanaka, S. Oda, M. Shiro, *Chem. Commun.* **2008**, 820–822; b) K. Tanaka, K.-I. Otani, *New J. Chem.* **2010**, *34*, 2389; c) L. Ma, J. M. Falkowski, C. Abney, W. Lin, *Nat. Chem.* **2010**, *2*, 838–846; d) C. D. Wu, A. Hu, L. Zhang, W. Lin, *J. Am. Chem. Soc.* **2005**, *127*, 8940–8941; e) K. Mo, Y. Yang, Y. Cui, *J. Am. Chem. Soc.* **2014**, *136*, 1746–1749; f) J. M. Falkowski, T. Sawano, T. Zhang, G. Tsun, Y. Chen, J. V. Lockard, W. Lin, *J. Am. Chem. Soc.* **2014**, *136*, 5213–5216.

[9] a) C. Martí-Gastaldo, D. Antypov, J. E. Warren, M. E. Briggs, P. A. Chater, P. V. Wiper, G. J. Miller, Y. Z. Khimyak, G. R. Darling, N. G. Berry, M. J. Rosseinsky, *Nat. Chem.* **2014**, *6*, 343–351; b) T. Kaczorowski, I. Justyniak, T. Lipińska, J. Lipkowski, J. Lewiński, *J. Am. Chem. Soc.* **2009**, *131*, 5393–5395.

[10] a) S. M. Cohen, *Chem. Rev.* **2012**, *112*, 970–1000; b) Y. Chen, V. Lykourinou, C. Vetromile, T. Hoang, L. Ming, R. W. Larsen, S. Ma, *J. Am. Chem. Soc.* **2012**, *134*, 13188–13191; c) B. Li, Y. Zhang, D. Ma, T. Ma, Z. Shi, S. Ma, *J. Am. Chem. Soc.* **2014**, *136*, 1202–1205; d) D. T. Genna, A. G. Wong-Foy, A. J. Matzger, M. S. Sanford, *J. Am. Chem. Soc.* **2013**, *135*, 10586–10589; e) P. Deria, J. E. Mondloch, E. Tylianakis, P. Ghosh, W. Bury, R. Q. Snurr, J. T. Hupp, O. K. Farha, *J. Am. Chem. Soc.* **2013**, *135*, 16801–16804; f) H. Jiang, B. Liu, T. Akita, M. Haruta, H. Sakurai, Q. Xu, *J. Am. Chem. Soc.* **2009**, *131*, 11302–11303.

[11] D. W. C. MacMillan, *Nature* **2008**, *455*, 304–308.

[12] a) S. Saito, H. Yamamoto, *Acc. Chem. Res.* **2004**, *37*, 570 – 579; b) K. Brak, E. N. Jacobsen, *Angew. Chem. Int. Ed.* **2013**, *52*, 534 – 561; *Angew. Chem.* **2013**, *125*, 558 – 588.
[13] M. Nakadai, S. Saito, H. Yamamoto, *Tetrahedron* **2002**, *58*, 8167 – 8177.
[14] a) R. Custelcean, M. G. Gorbunova, *J. Am. Chem. Soc.* **2005**, *127*, 16362 – 16363; b) T. Devic P. Horcajada, C. Serre, F. Salles, G. Maurin, B. Moulin, D. Heurtaux, G. Clet, A. Vimont, J.-M. Grenèche, B. L. Ouay, F. Moreau, E. Magnier, Y. Filinchuk, J. Marrot, J.-C. Lavalley, M. Daturi, G. Férey, *J. Am. Chem. Soc.* **2010**, *132*, 1127 – 1136; c) C. Volkringer, T. Loiseau, N. Guillou, G. Férey, M. Haouas, F. Taulelle, E. Elkaim, N. Stock, *Inorg. Chem.* **2010**, *49*, 9852 – 9862; d) T. Gadzikwa, O. K. Farha, K. L. Mulfort, J. T. Hupp, S. T. Nguyen, *Chem. Commun.* **2009**, 3720 – 3722; e) Q. Yang, S. Vaesen, F. Ragon, A. D. Wiersum, D. Wu, A. Lago, T. Devic, C. Martineau, F. Taulelle, P. L. Llewellyn, H. Jobic, C. Zhong, C. Serre, G. D. Weireld, G. Maurin, *Angew. Chem. Int. Ed.* **2013**, *52*, 10316 – 10320; *Angew. Chem.* **2013**, *125*, 10506 – 10510.
[15] X. Xi, Y. Fang, T. Dong, Y. Cui, *Angew. Chem. Int. Ed.* **2011**, *50*, 1154 – 1158; *Angew. Chem.* **2011**, *123*, 1186 – 1190.
[16] CCDC 899848 (**1**), 899849 (**2**), and 899850 (**3**) contain the supplementary crystallographic data for this paper. These data can be obtained free of charge from The Cambridge Crystallographic Data Centre via www.ccdc.cam.ac.uk/data_request/cif.
[17] A. L. Spek, *J. Appl. Crystallogr.* **2003**, *36*, 7 – 13.
[18] W. Notz, F. Tanaka, C. F. Barbas, *Acc. Chem. Res.* **2004**, *37*, 580 – 591.
[19] a) J. Horn, F. Michalek, C. C. Tzschucke, W. Bannwarth, *Top. Curr. Chem.* **2004**, *242*, 43 – 75; b) D. Font, C. Jimeno, M. A. PericPs, *Org. Lett.* **2006**, *8*, 4653 – 4655.
[20] a) F. Vermoortele, R. Ameloot, A. Vimont, C. Serre, D. De Vos, *Chem. Commun.* **2011**, *47*, 1521 – 1523; b) S. Horike, M. Dinca, K. Tamaki, J. Long, *J. Am. Chem. Soc.* **2008**, *130*, 5854 – 5855.

